We are IntechOpen, the world's leading publisher of Open Access books Built by scientists, for scientists

4,800
Open access books available

122,000
International authors and editors

135M
Downloads

Our authors are among the

154
Countries delivered to

TOP 1%
most cited scientists

12.2%
Contributors from top 500 universities

CLARIVATE ANALYTICS BOOK CITATION INDEX INDEXED

WEB OF SCIENCE™

Selection of our books indexed in the Book Citation Index in Web of Science™ Core Collection (BKCI)

Interested in publishing with us?
Contact book.department@intechopen.com

Numbers displayed above are based on latest data collected.
For more information visit www.intechopen.com

1

Study of CrAlN Multilayred Thin Films

Tlili Ibrahim[1] and Taher Ghrib[2]
[1]*Laboratoire Bourguignon des Matériaux et Procédés (LaboMap), CER ENSAM de Cluny 71250*
[2]*Technopole Borj Cedria*
[1]*France*
[2]*Tunisia*

1. Introduction

The optimization of mechanical and tribological properties of monolayer coatings developed and studied is a way of reaching and important research, because of their potential application in various mechanical fields. Hardness and tenacity are the first two principal characteristics of the deposits which it is necessary to optimize them to improve their wear resistance. From this, the layers Cr, CrN and CrAlN are superimposed with different levels of constraints residual (Pc, Pt or combined) to obtain multilayer coatings that fulfill better the industrial requirements.

The characterizations microstructural, morphological and physicochemical of the various multi-layer coatings are essential within the framework of this study, of which the objective is it to connect the mechanical properties of these deposits to their macroscopic and microscopic study.

A variety of multilayer systems such as TiN/CrN [1], TiAlN/CrN [2], TiN/TiAlN [3], etc., have been studied extensively. However, there are very few reports on the multilayer coatings based on CrN and CrAlN [4]. The addition of Al to CrN system permits to work at higher temperatures where the oxidation occurs [5]. CrAlN coatings have been reported to be stable up to a temperature of 900°C depending upon the Al content in the coatings [6]. CrAlN coatings also exhibit higher hardness and a lower friction coefficient compared to CrN coatings [7]. The new ternary film structure brought about significant advances in coating designs, such as the decrease of the grain size and the formation of grain boundaries between the two phases. As a consequence, it is reported that CrAlN films exhibited excellent mechanical properties and oxidation resistance owing to their solid solution structure [8]. Furthermore, it is well known that most properties of these solid solution composite films are influenced by certain factors such as crystalline structure and micro-structure. These factors led to the study of the multilayers coatings of CrN/CrAlN and Cr/CrN/CrAlN, in which the properties of Cr, CrN and CrAlN can be combined. The Cr underlayer is considered as a bonding layer.

In this work, we have investigated the effect of thickness on residual stress and hardness of the monolayers. Moreover, the relationship between mechanical properties and the stress state of the multilayers coatings was also discussed and established.

2. Structural, microstructural and morphological characterization

By taking account of the optimal conditions obtained on the mono-layers, we developed six multi-layers coatings Cr/CrN/CrAlN and CrN/CrAlN with various residual stresses levels in mono-layers which constituents them.
The films composition, thickness and roughness are given respectively by the EDS or WDS analysis and the 3d optical profilmeter. (fig. 1).
The analysis carried out on the multi-layer coatings Cr/CrN/CrAlN or CrN/CrAlN shows the homogeneity of various chemical compositions at the several surface points, the principal characterizations results carried out are given in table 1.
According to analyses EDS one found that in the studied coatings the N/Cr report/ratio is about 1.17 to 1.2 and that they contain only 2.2% atomic of oxygen to the maximum. The roughness of films is characterized by two parameters (Ra and Rt) whose measured values are high, which leads us to await a dispersion of hardness by tests of nano indentation.
Concerning the analysis by DRX (fig. 2), one will limit the study on the films PVD_1 and PVD_4 since the total thickness of other films is low (< 35nm).
These multi-layers is elaborate with low internal stresses (Pt). The coating PVD_4 is presented by the peaks of principal diffraction [(111) and (200) respectively with 36.8° and 51.27°, to compare with file PDF 76-2494, PCPDFWIN version 2.3, JCPDS-ICDD (2002)] [9]. The addition of an under-layer Cr to the coating PVD_4 one obtains the film PVD_1 and this gives a peak to position $2\theta = 43.6°$ allotted to the presence of a cubic phase CrN (111) identical to the ref [9-11].
In addition, it is established that the peaks Cr_2 NR (111) and CrN (200) are confused they is because of the effect of under-stoechiometric coatings. Another remark, one can conclude according to the spectra obtained on the multi-layers PVD_1 and PVD_4 that the CrN layer crystallizes on the surface according to the preferential orientation (311) whereas it crystallizes in volume according to the preferential orientation (200) [12]. The quantitative

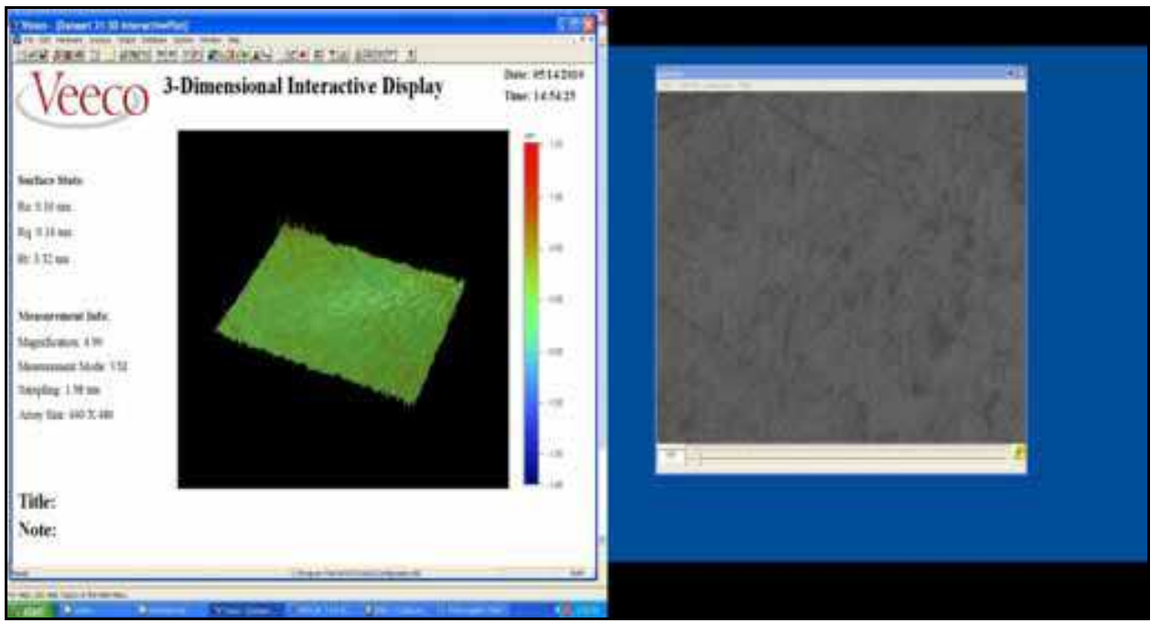

Fig. 1. Topography of coating PVD_1 obtained by the optical profilometer.

Revêtements	N (at. %)	Al (at. %)	Cr (at. %)	N/Cr	Total thickness (nm)	Rugosité (µm)	
						Rugosité arrithmétique (R_a)	Quadratic roughness (R_q)
Cr/CrN/CrAlN ($P_t/P_t/P_t$):PVD$_1$	51.8	4.2	42.9	1,2	1500	0.1	0.14
CrN/CrAlN (P_t/P_c):PVD$_2$	50.8	4	43.1	1.17	300	0.12	0.16
Cr/CrN/CrAlN ($P_t/P_c/P_c$):PD$_3$	50.5	4.7	42.5	1.18	300	0.11	0.15
CrN/CrAlN (P_t/P_t):PVD$_4$	52	5	41.3	1.2	1500	0.13	0.15
CrN/CrAlN (P_c/P_c):PVD$_5$	49.7	4.9	43.6	1.18	256	0.12	0.16
Cr/CrN/CrAlN ($P_c/P_c/P_c$):PVD$_6$	50.1	4.2	44.5	1.17	356	0.09	0.13

Table 1. Chemical composition and topography

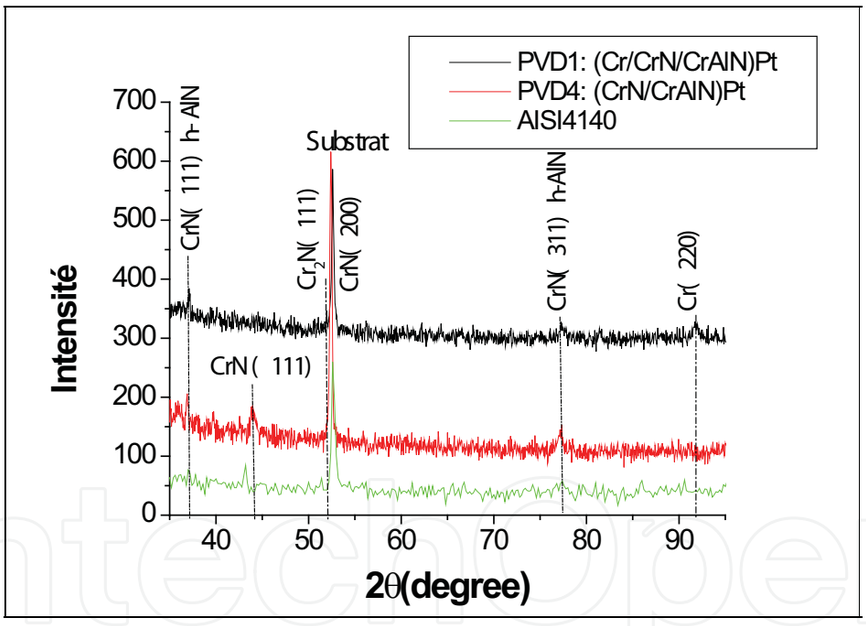

Fig. 2. Diffraction spectra of x-rays obtained with the multi-layer PVD1, PVD4 and steel 42CrMo4.

analysis of the layer revealed the coexistence of the CrN phases and Cr2N, this result is confirmed by C Nouveau [13, 14]. An observation in HRTEM and diffraction stereotype confirmed the presence of a mixture of CrN (200) phases in the Cr2N layer.

We remark that by adding a Cr underlayer to the PVD_4 coating, the peak CrN (111) disappeared completely.

This can be explained by the fact why the plans (311) have a speed of growth more significant than the plans (111) and by preferential pulverization of the atoms of nitrogen of the plans (111) compared with those of the plans (311).

In addition, the presence of a crystallographic structure is related to the column-like morphology of the mono-layers Cr, CrN and CrAlN observed by SEM on a cross section after a polishing mirror (fig. 3).
The growth of the structure in columns took place perpendicular to surface. The found results are comparable with that obtained in work of Harish C. Barshilia and M. Okumiya, M. Griepentrog [15, 16] carried out on the CrN/CrAlN layers.
In order to conclude this study from obtaining the multi-layers, have determined the profiles of the chemical compositions versus the pulverization time (fig. 4). The interface

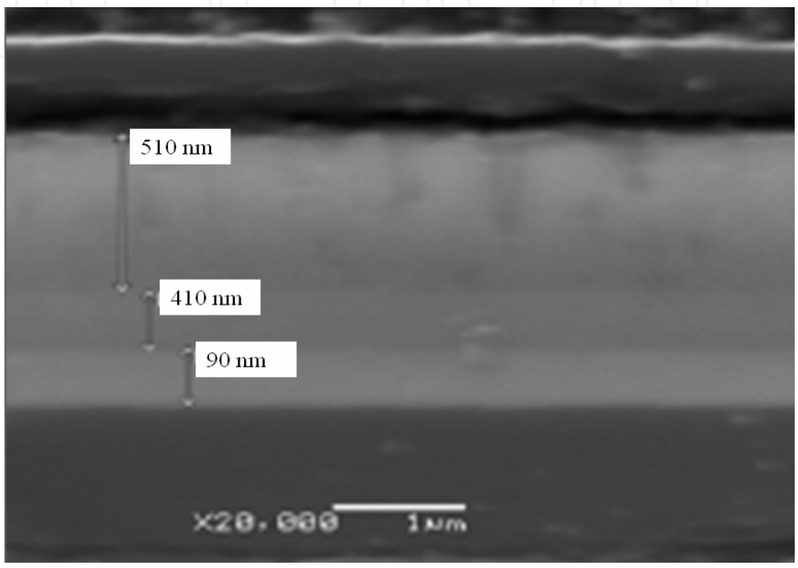

Fig. 3. SEM of a transverse cut followed by a polishing mirror coating Cr/CrN/CrAlN.

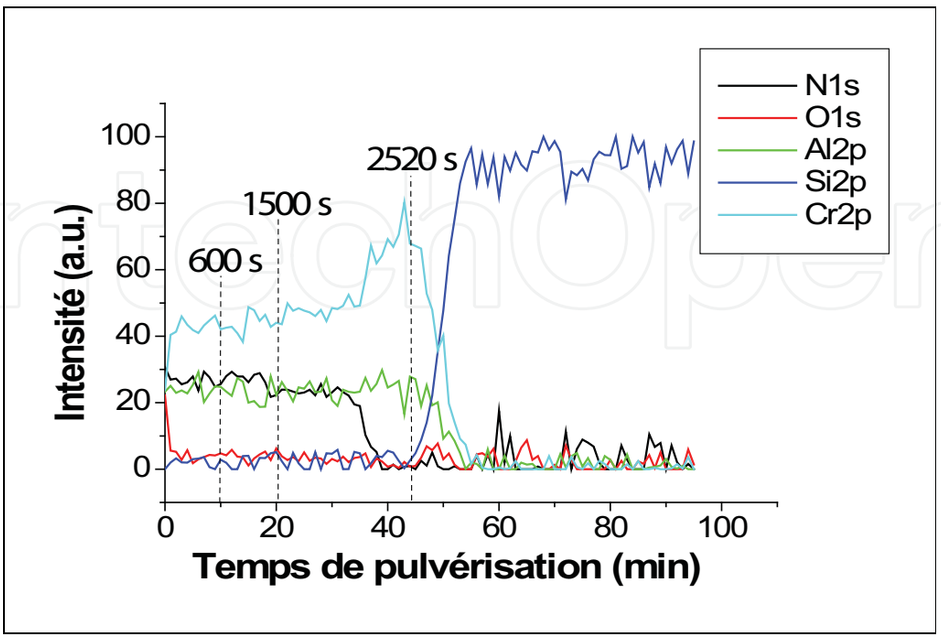

Fig. 4. Compositions Profiles of the Cr/CrN/CrAlN layer obtained by XPS.

between the individual layers is not very clear, which proves that these layers are very miscible. Moreover, there is a contamination of surface of this coating is highlighted by the presence of species oxidized of chromium on a depth of a few tens of nanometers. Aluminium is presented by a small proportion in the surface of CrAlN layer with 5% which imply that it is not possible to distinguish the variation from its profile in the film.
By taking account dimensions of the aluminium atoms and its kinetic energy. It is well doped in the CrN layer, which to allow him to reach a significant depth, from where the interface between the two layers CrN/CrAlN is not remarkable. The profile of the flexible layer (Cr) is more intense close to the interface layer/substrat which is coherent with the superposition of muti-layers (Cr/CrN/CrAlN) on silicon. The interface is relatively narrow and the involved species do not seem to penetrate in the substrate what attests the layer good quality.
One selected two moments over the pulverization time (600s and 1500s), of which the goal to know the evolution of the specific spectrum of the studied multi-layer Cr/CrN/CrAlN. The Fig. 5 (1) schows that spectra N_{1s} of the studied layer revealed the presence of a characteristic peak of chromium nitride centered at 397 eV. This result is found in the references [17 - 18]. The width with middle height (WHM) for the two moments 600s and 1500s is about 1.45 eV and 1.62 eV respectively.

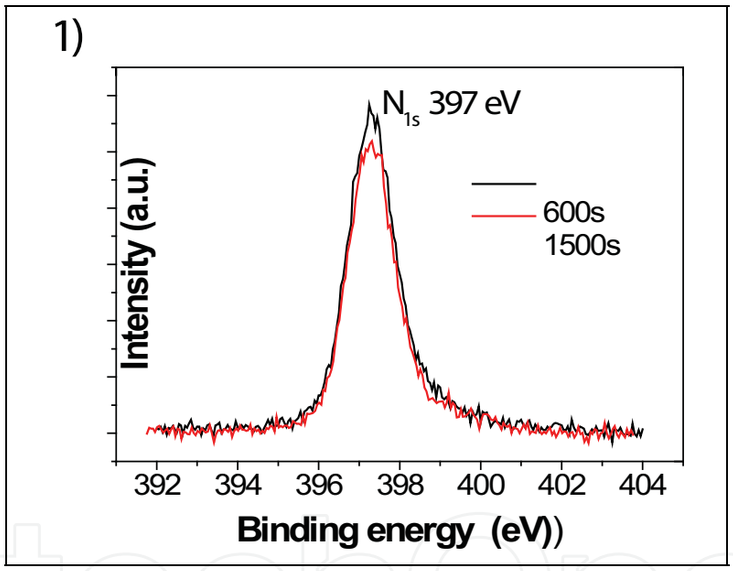

Fig. 5.1.

The binding energy corresponds to the peak O_{1s} is 531.5 eV, and the width with middle height is about 2 eV (fig. 5 (2)) for the two moments.
The peak associated to Cr (fig. 5(3)) is composed of two peaks centered at 574,8 and 584 eV, who correspond to Cr $_{2P3/2}$ and Cr $_{2P1/2}$ respectively.
The widths with middle height (FWHM) for the two peaks are measured in the two selected moments, 600 and 1500 and the values obtained are as follows: the peak $Cr_{2P3/2}$ (1.3 and 2.3) and the peak Cr $_{2P1/2}$ (2.25 and 2.75), respectively.
The spectra Al_{2p} and Cr_{3s} (fig. 5(4)) are confused and the corresponding binding energy is 74.3 eV [15, 18 - 20]. The width with middle height is 3.75eVand 4.2eV for 600s and 1500s respectively.
Investigations XPS on the figure I.1f, shows the presence of the elements O, N, Al and Cr in the Cr/CrN/CrAlN coating. From the intensity of the peaks N_{1s}, O_{1s}, Cr_{2p} and Al_{2p} + Cr_{3s},

we can estimate the film composition. There is oxygen with a feeble proportion (< 3%) in the coating. coherent with the results obtained by WDS, it is attributed to the incorporation of

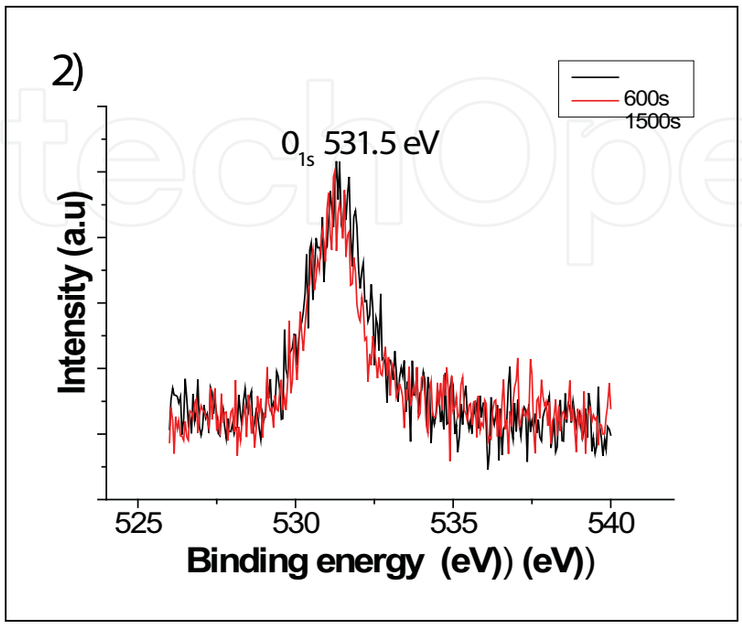

Fig. 5.2.

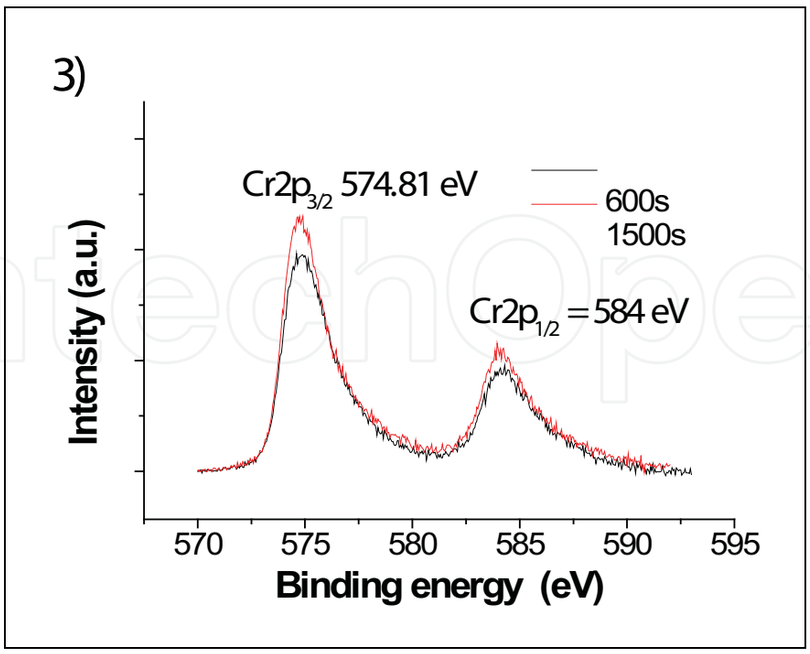

Fig. 5.3.

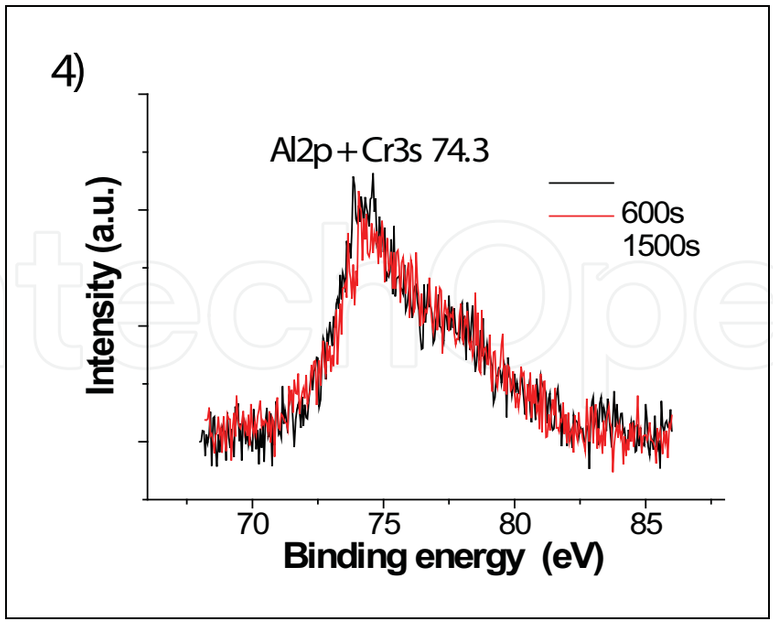

Fig. 5.4.

oxygen in plasma during the pulverization of the target of Cr. These results are coherent with the other work completed by Lappitz and Hubert [20]. The narrow spectrum of metal chromium is for 574.81 eV, but its incorporation with nitrogen changes the spectrum with 575.7±0.5 eV [21]. The origin of this change in fact that the film of nitride is composed of phases mixture like CrN, Cr_2N, CrN_xO_y and $CrN(O_2)_x$.

The peak O_{1s} relates to chromium oxides Cr_2O_3 and CrO_3 [21]. The analysis by atomic force microscopy AFM of a surface section for each multi-layer makes it possible to determine the morphology properties of the Cr/CrN/CrAlN and CrN/CrAlN coating (fig. 6). Surfaces are

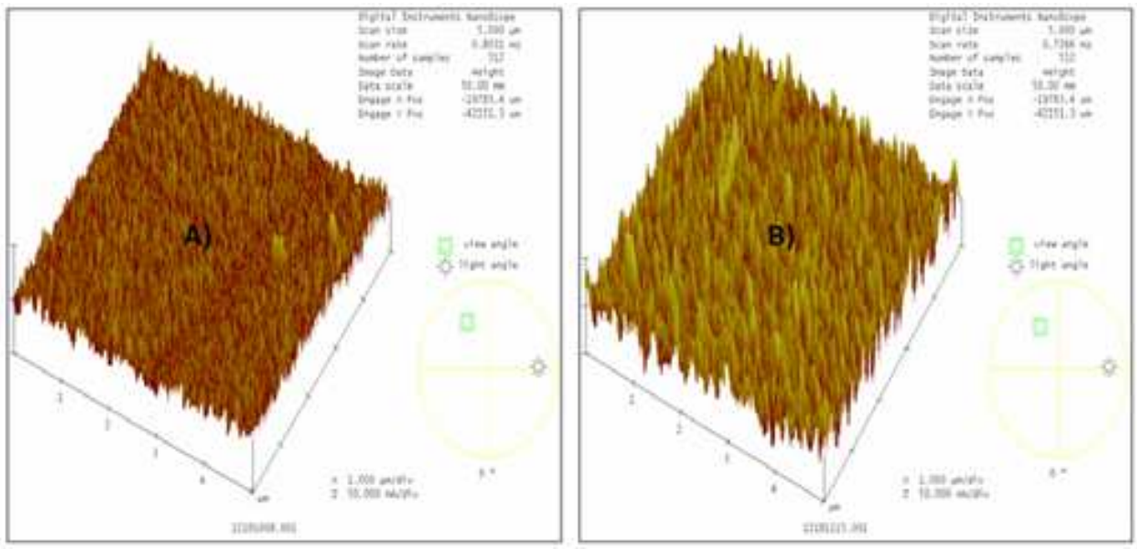

Fig. 6. Morphologies of the multi-layer coatings obtained by AFM: A) CrN/CrAlN and B) Cr/CrN/CrAlN.

generally uniform, they present domes and peaks of which average radii and the maximum height are respectively about 150 and 41 nm for Cr/CrN/CrAlN, and approximately of 178 and 26 nm for CrN/CrAlN. In addition the roughness of surface is characterized by the parameters Ra and Rz who are in order 7.18 and 25.85 nm for CrN/CrAlN (fig 7-A), and 12.31 and 40.83 nm for Cr/CrN/CrAlN (fig 7-B). Following this analysis one can say that the CrN/CrAlN coating has a structure finer than that of the Cr/CrN/CrAlN coating. Thus, the morphology of CrN/CrAlN is characterized by a denser and uniform structure.

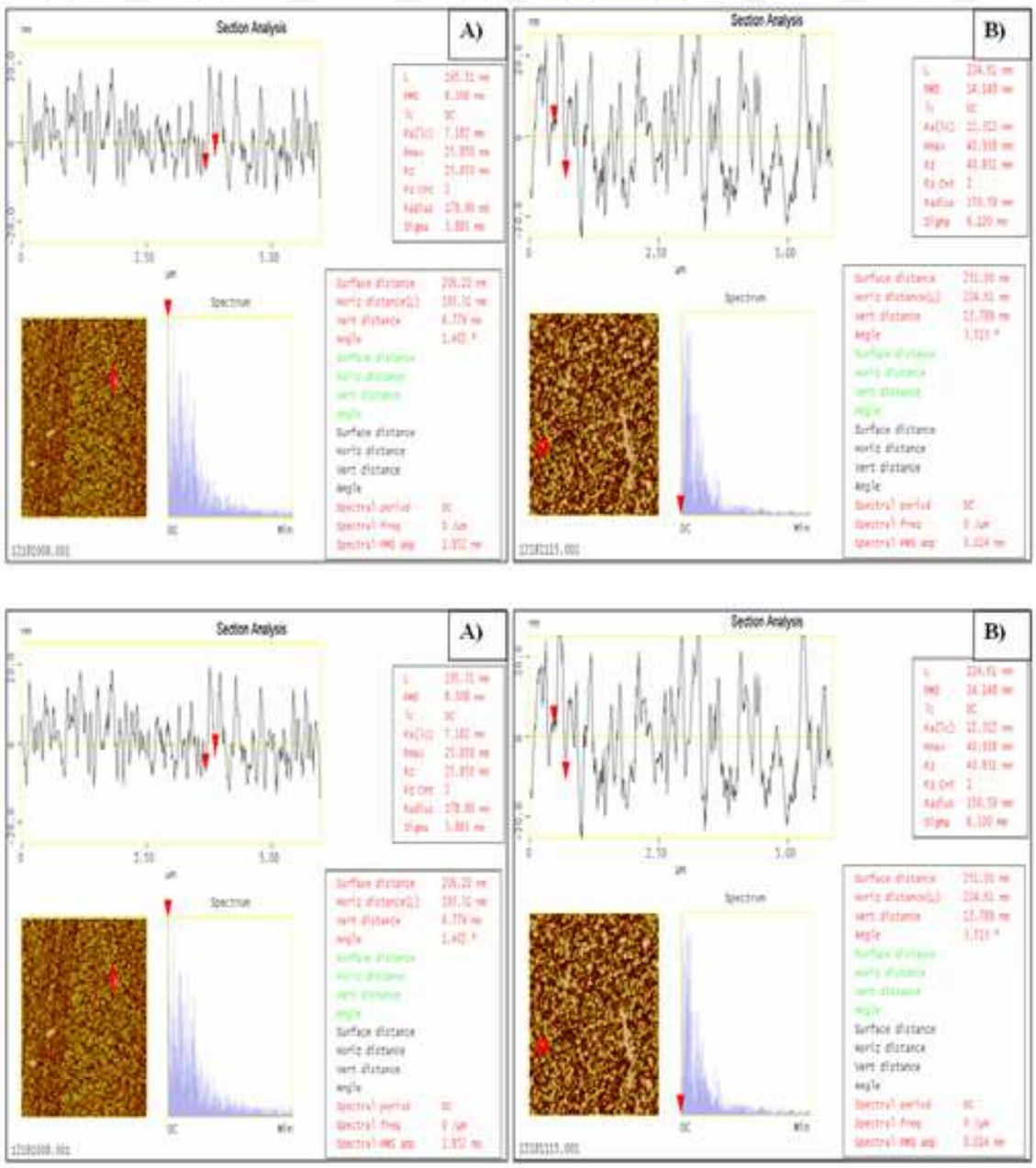

Fig. 7. Analyze by x AFM of a multi-layer section coatings:
A) CrN/CrAlN and B) Cr/CrN/CrAlN.

2. Thermal properties

2.1 Principle of the PTD technique

The thermal properties such as the thermal conductivity and the thermal properties are determined by the PTD technique. This method consists in heating a sample with a modulated light beam of intensity $I = I_0(1+\cos\omega t)$. The thermal wave generated by the optical absorption of the sample will propagate in the sample and in the surrounding fluid (air in our case). The thermal wave in the fluid will induce a temperature gradient then a refractive index gradient in the fluid which will cause the deflection ψ of a probe laser beam skimming the sample surface. This deflection may be related to the thermal properties of the sample. The sample is a stack of n layers, we write the heat equations in these areas and in the two surrounding fluids which are the air in by designating K_i , D_i and l_i, respectively the thermal conductivity, the thermal diffusivity, and the thickness of the layer i (Fig.8).

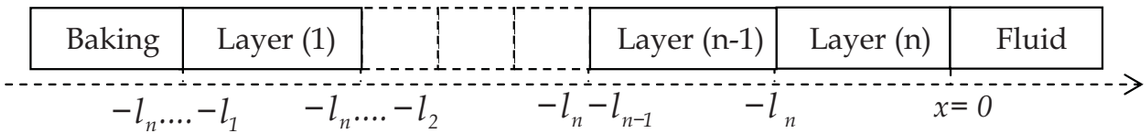

Fig. 8.

2.2 Theoretical model

In the case of an uniform heating we can use a 1-dimensional approximation, and the amplitude $|\psi|$ and phase φ of the probe beam deflection ψ are given by:

$$|\psi| = \frac{\sqrt{2}\ L}{n\ \mu_f}\frac{dn}{dT_f}|T_0|e^{-\frac{x}{\mu_f}} \quad \text{and} \quad \varphi = -\frac{x}{\mu_f}+\theta+\frac{5\pi}{4}$$

Where l is the width of the pump beam in the direction of the probe laser beam, n, μ_f and T_f are respectively the refractive index, the thermal diffusion length and the temperature of the fluid.. $|T_0|$ and θ are respectively the amplitude and phase of the temperature T_0 at the sample surface which are function of the thermal properties of the different media, and x is the distance between the probe beam axe and the sample surface.

Before the calculation of the probe beam deflection, one must know the expression of the surface temperature T_0 that obtained by writing the temperature and heat flow continuity at the interfaces $x_i = -l_n - l_{n-1} ... - l_i$:

$$T_0 = \left[((1+b)\,\eta_4 e^{\sigma_1 l_1} - (1-b)\eta_2 e^{-\sigma_1 l_1})E_n + (r_1 - b)\,e^{-\alpha_1 l_1}E_1\right] \Big/ \left[(1-b)\eta_1\ e^{-\sigma_1 l_1} - (1+b)\,\eta_3 e^{\sigma_1 l_1}\right]$$

With

$$E_i = \frac{\alpha_i}{2K_i(\alpha_i^2-\sigma_i^2)}, \sigma_i = (1+j)\sqrt{\frac{\pi\ f}{D_i}} \quad , \ b = \frac{K_b\sigma_b}{K_1\sigma_1} \quad , \ g = \frac{K_f\sigma_f}{K_n\sigma_n} \ et\ \ r_1 = \frac{\alpha_1}{\sigma_1}$$

and η_1 , η_2 , η_3 , η_4 are constant whose expressions depend on thermal properties and numbers of layers [17].

2.3 Experimental set-up

The sample is heated by an halogen lamp light of power 100W modulated thanks a mechanical chopper at a variable frequency (Fig. 9). A He-Ne laser probe beam skimming the sample surface at a distance z is deflected. This deflection can be detected by a four quadrant photo-detector and converted to an electrical signal which is measured by a lock-in amplifier. Through the intermediary of interfaces, the mechanical chopper and the lock-in amplifier a microcomputer will set the desired modulation frequency and read the values of the amplitude and phase of the photothermal signal and then draw their variations according to the square root modulation frequency.

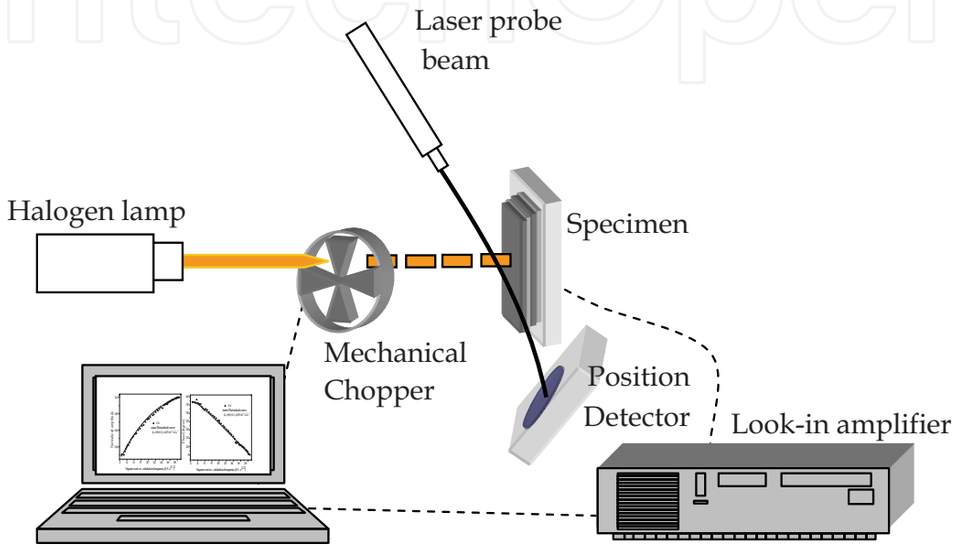

Fig. 9. Experimental set-up

2.4 Determination of the thermal properties

By applying the model developed with N layers to our coatings multi-layer Cr/CrN/CrAlN, Cr/CrN and mono-layer Cr by taking account of the thickness of each layer constituting the coating [22,23]. The obtained experimental results are presented by the figures 10-a, b, c. The thermal properties of each layer are deduced when there is a coincidence between the experimental and theoretical curves.
The results obtained are given in the table 2:

Revetment	Thermal conductivity ($W.m^{-1}.K^{-1}$)	Thermal diffusivity ($10^{-4}m^2.s^{-1}$)	Equivalent thermal Conductivity ($W.m^{-1}.K^{-1}$)
Cr	93,9	0,79	
CrN	11	0,23	
CrAlN	2.8	0,052	
Cr/CrN			13.1
Cr/ CrN/CrAlN			4.6

Table 2. Thermal properties of different multi-layer.

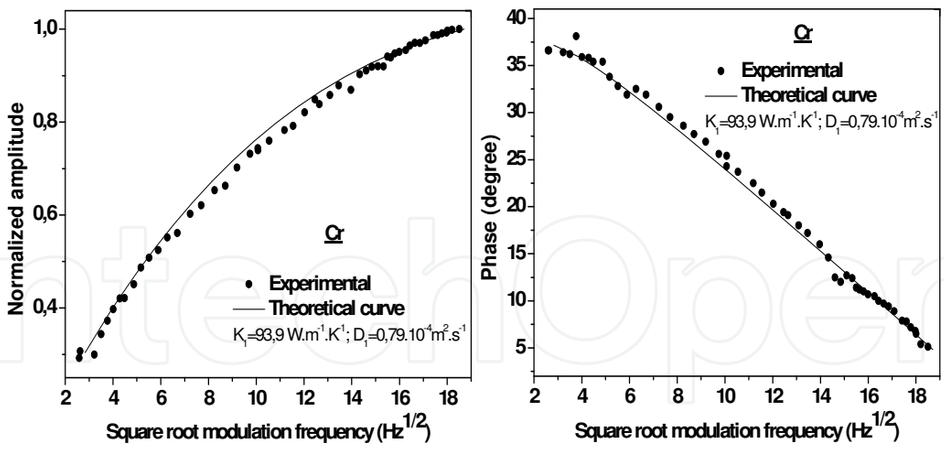

(a)

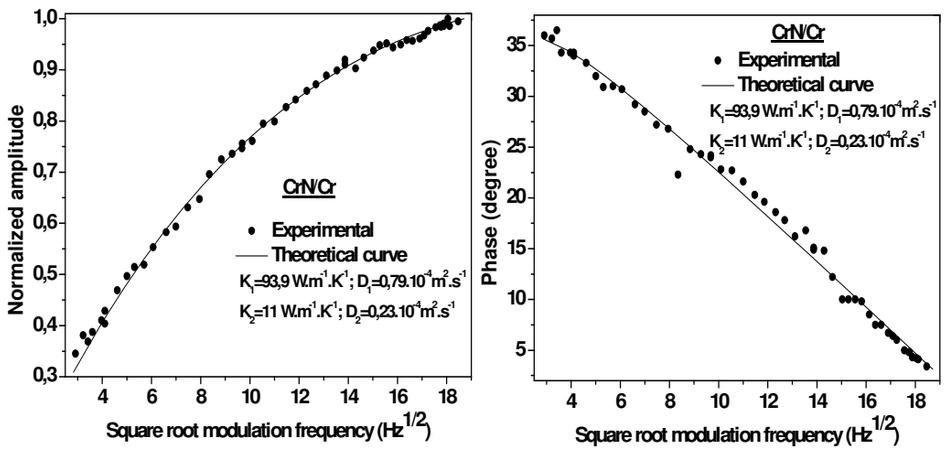

(b)

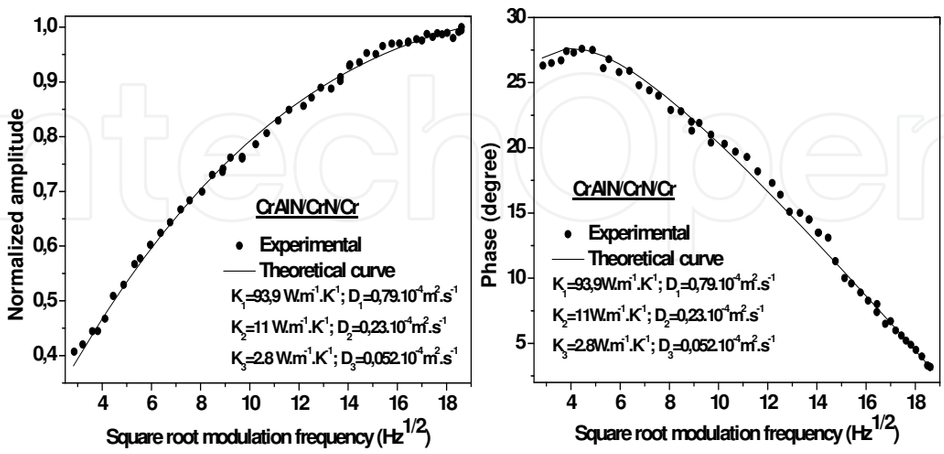

(c)

Fig. 10. Amplitude and phase of the signal for a sample of Silicon on which is deposited the coatings: a) Cr, b) Cr/CrN et c)Cr/CrN/CrAlN

These values show that the thermal properties of the CrAlN layer are weak, compared to the CrN layers and Cr taken separately, therefore it can act like a heat insulator. That can be explained by a column microstructure which is characterized by the lengthened shape of the pores inter-column-like which are mainly aligned perpendicular to the plan of the layer [24,25], and since the heat flow is primarily parallel to these gaps inter-columns, the transfer of heat is effectively significant. These fine gaps inter-column-like contribute to a moderate reduction of thermal conductivity and are generally opposed to the heat propagation.

For this reason, the thermal conductivity of the CrN. layer is also clearly lower than the thermal conductivity of the Cr layer which is dense. This result suggests that the structure of coatings Cr and CrN close to the interface to the metal substrate have a very different thermal conductivity. The difference in the structure of multi-layer coatings Cr/CrN / CrAlN and Cr/CrN can coarsely be divided into two zones, the interior zone with fine grains (CrN/Cr) and the zone external with large columns (CrAlN). The thermal conductivity of the interior zone with fine grain is much higher than the thermal conductivity of the external zone.

Thermal conductivity is dominated by the defect of the grain boundary in this part of the coating, it results from it a lower conductivity of about 2,5 $W.m^{-1}.K^{-1}$ at the ambient temperature.

Moreover, the reduction in the thermal conductivity of the multi-layer coating Cr/CrN/CrAlN is allotted to the increase in total porosity, We can conclude for thin films that the thermal conduction is a comprehensive process, which is due to the vibration of the crystal lattice, and the realization of a stacking of several layers provide a thermal conductivity which verifies the general relationship $\frac{1}{K}=\frac{1}{l}\sum_i \frac{l_i}{K_i}$, where l and K are respectively the total thickness and the equivalent conductivity of the stack; l_i and K_i are respectively the thickness and thermal conductivity of different layers constituting the stack.

3. Study of the mechanical characteristics

3.1 Residual stresses

A similar study of the residual stresses is carried out on the multi-layer coatings.

Fig. 11, shows that the residual stresses in the multi-layers are lower than those of constituent mono-layers.

This reduction of the residual stresses is mainly du to the interfaces created between the various superposed layers. Indeed, the total constraint is 3.4 times higher if one compares PVD_1 (all the mono-layers are with P_t) with PVD_6 (all the mono-layers are with P_c). The value of the highest constraints is obtained in multi-layer PVD_6. In addition, the same results are obtained when one compares PVD_4 and PVD_5; the constraints are also increased by 3.5 times. In fact, if one compares multi-layer PVD_1 and PVD_4 or PVD_5 and PVD_6, it is obvious that the underlayer of Cr has a major effect, because the connection Cr of the layer, has exploited a principal role in the constraints intensity, what proves that the level of these constraints on the coating PVD_6 (-1.2 GPa) is higher than in PVD_5 (- 0.7GPa). We can also note that if one compares PVD_2 and PVD_5, the level of the constraints remains almost the same whatever the state of stress in the CrN layer (~ 0.65 - 0.7GPa).

These results mean that the underlayer, Cr or CrN improves the constraints intensity of these multi-layer that if they are at their point P_T as the surface layer. If not, if the underlayers are at their P_T point and the surface layers at their P_c point, then the increase in constraints is due to the fact that these layers have their highest constraints. Lastly, these results would be interesting in the choice of multi-layer according to their later applications (mechanical, thermal, wear, etc...).

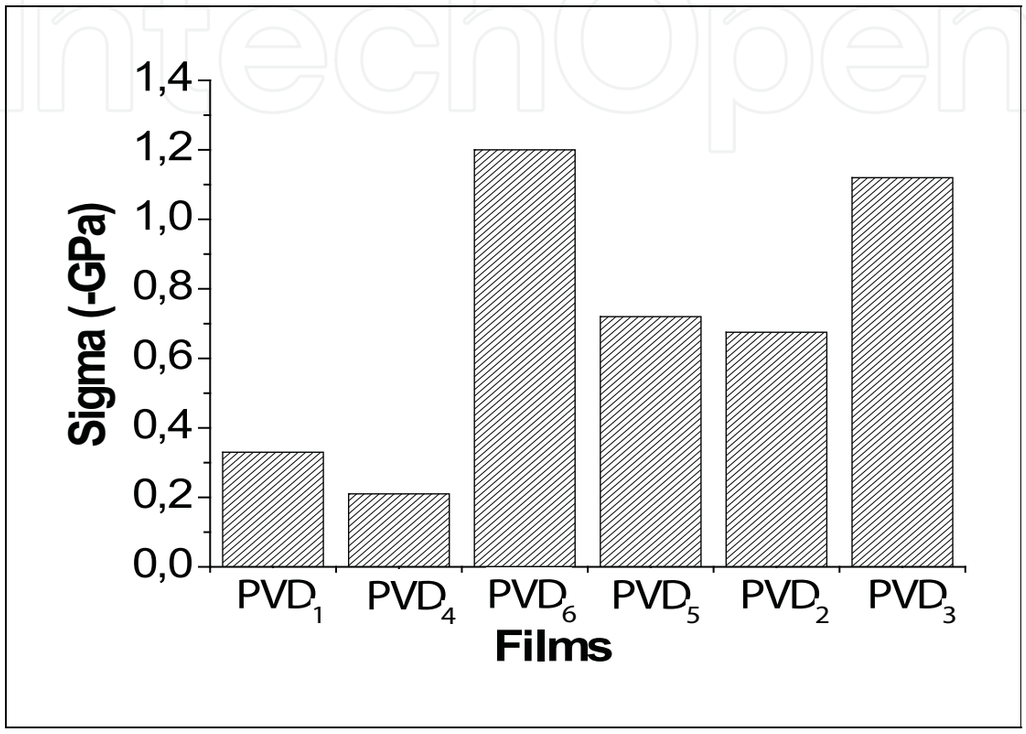

Fig. 11. Multi-layers Residual stresses

3.2 Adhesion

Tests of scratching are carried out by scratch-test on the six multi-layer coatings (fig. 12).
The films are compared two to two according to their total thicknesses and of level of the residual stresses (P_T and P_c) in the mono-layers. The stripes of various films are studied and investigated.
Generally, all the films have an average adherence with the substrate steel of $42CrMo_4$
Exceptionally PVD_1 has a high adherence characterized by a critical effort F_c = 78 N (fig II.2a). This fact, whatever the level of the residual stresses (P_t, P_c or combined) of the mono-layers, good adherence in films is always associated to the presence of a fixing under-layer Cr : $Fc_{-PVD1} > Fc_{-PVD4}$; $Fc_{-PVD3} > Fc_{-PVD2}$ et $Fc_{-PVD6} > Fc_{-PVD5}$ (fig 12-a, b et c). These films PVD_1, PVD_3 and PVD_6 are also characterized by high residual stresses (fig. 11).
Analysis of this adherence performance can be connected to the rupture of the columns growth of the mono-layers and a propagation envisaged of the cracks will be limited only on the surface layers. If one takes account only to films thicknesses, the coatings PVD_3 and PVD_6 are less thick than PVD_1, on the other hand this last has a better adherence although

these coatings have the same constituent layers. It is known that if the thickness increases the adherence decreases, but the wear resistance increases. The greatest critical load associated with PVD_1 can be related to the reduction at the same time to the average intern energy and to the constraints to the interface of the mono-layer [24].

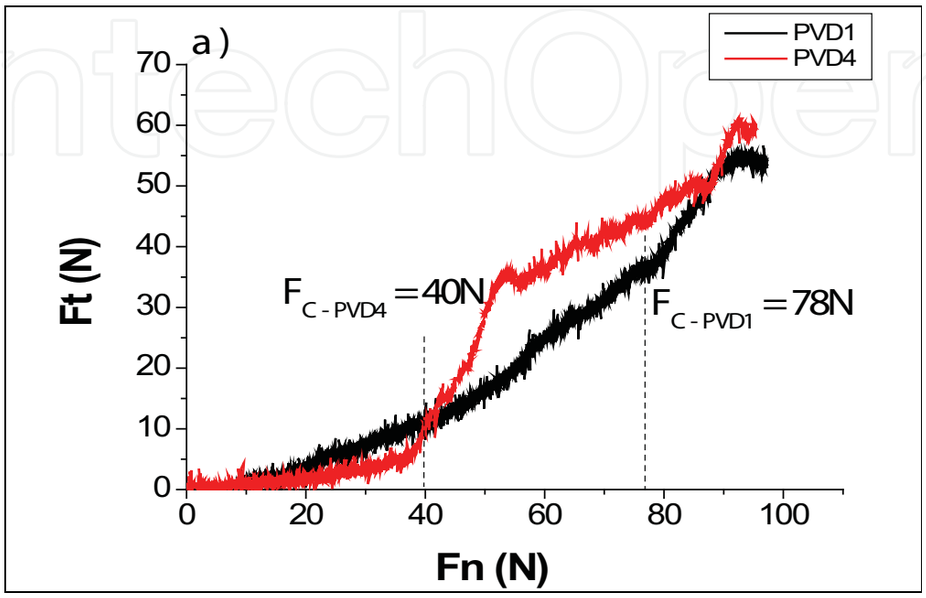

(a)

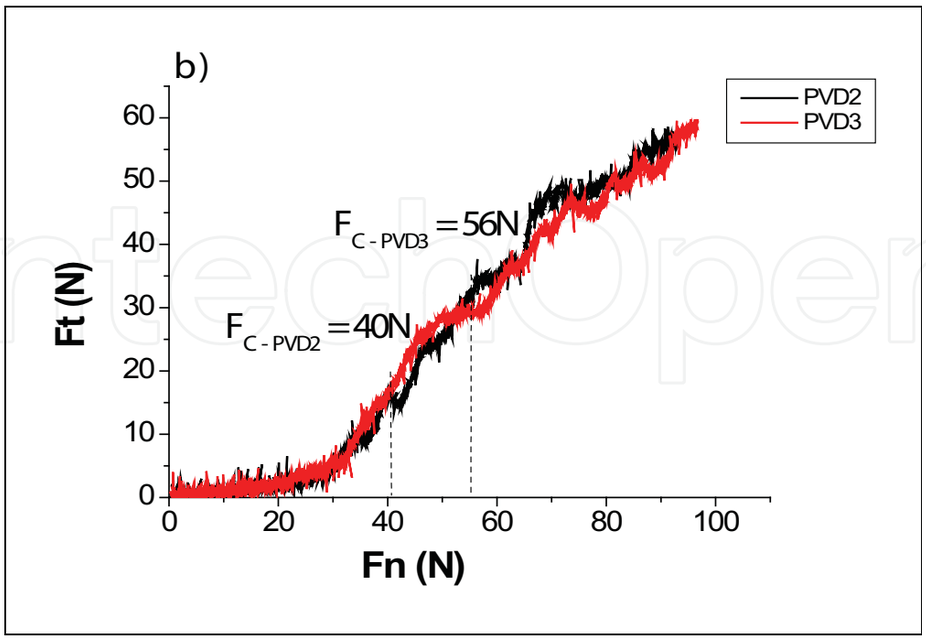

(b)

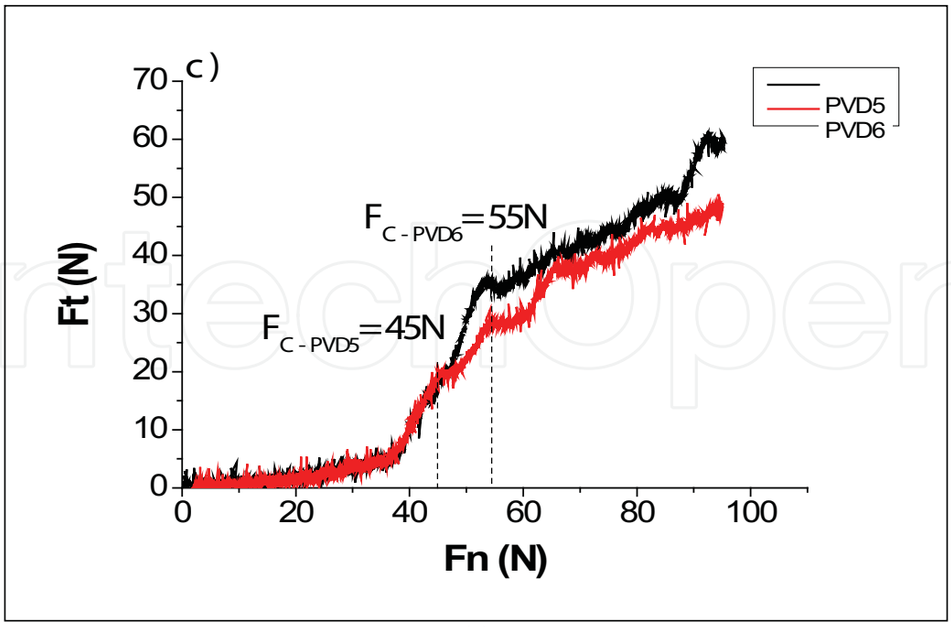

(c)

Fig. 12. Scratch-tests carried out on the multi-layers:
a) PVD_1 et PVD_4, b) PVD_2 et PVD_3 et c) PVD_5 et PVD_6

Moreover, if one takes account only for constraints levels in the mono-layers which constitute film. It is established that, more this level is weak P more the adherence is significant (table 3). On the other hand the absence of a flexible underlayer Cr in films supports a low adherence whatever the thickness and the constraints levels associated to the established coatings.

3.3 Study of behavior to wear

The wear of the various deposits is quantified by using the method of the average values in order to estimate the total profile of the worn surface. After each test of friction the damage creates is studied. By taking account of films thicknesses and roughness associated to their surfaces. Worn volumes of the coating and the basic substrate are given separately after each tribological test (fig 13-a). By comparing the wear of the films two to two and by taking account of the intensity of the residual stresses and film thickness, the multi-layer coatings developed with an underlayer Cr have a better wear resistance than those developed without this underlayer ($V_{PVD1} > V_{PVD4}$, $V_{PVD6} > V_{PVD5}$ and $V_{PVD3} > V_{PVD2}$).

Coatings	PVD1	PVD2	PVD3	PVD4	PVD5	PVD6
Fc (N)	78	40	56	40	45	55

Table 3. Adhesion Forces F_c of multi-layer deposited on steel 42CrMo4.

If one takes account only of the constraints intensity in the partial layers, constituent of film, it appears that when the constraints levels are combined (P_t and P_c), the film has a better wear resistance than those presented by levels P_t or P_c only, it is the case of the PVD_3 coating. So one can say that worn volume is proportional to the depth of wear for each tribological test and the results found on the wear depth are coherent with those found for worn volume. In addition, all the coatings improve the wear resistance compared to the basic substrate (42CrMo4).

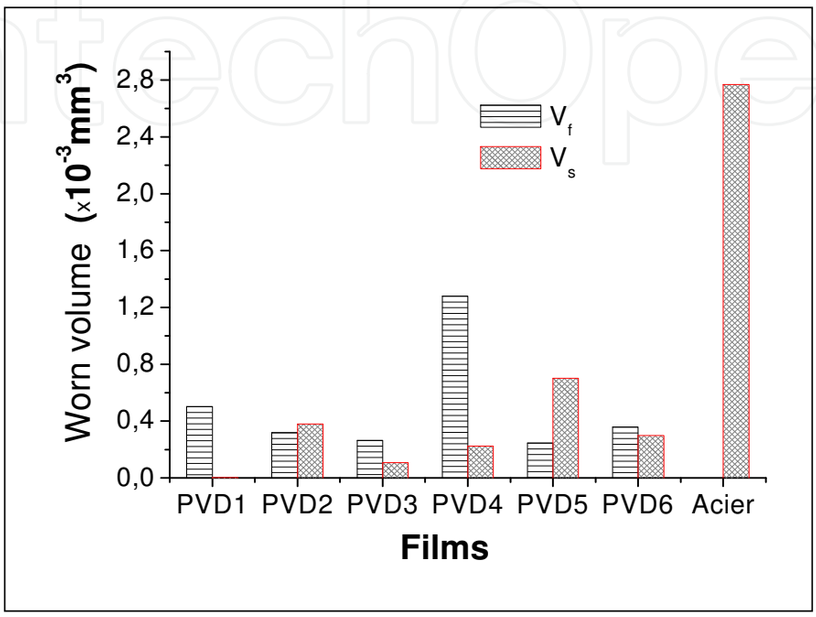

Fig. 13-a. Worn volume of the various multi-layer coatings: t = 15min, Fn = 5N et δ = 5mm

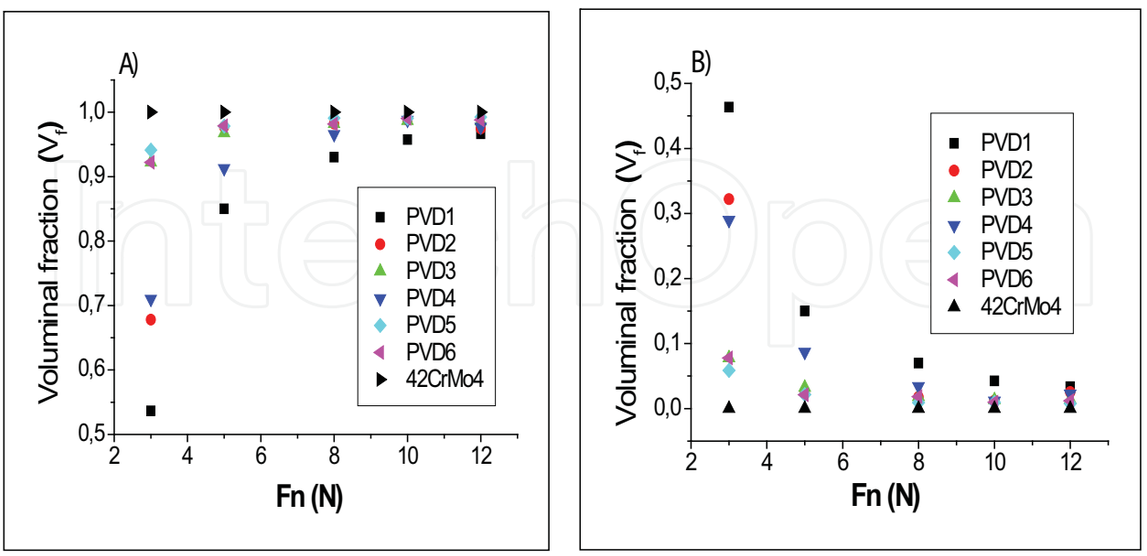

Fig. 13-b. Voluminal fraction of the multi-layer coatings and the substrate:
A) films and B) Substrate.

To study the influence of the operational parameters on the removed matter quantity, after each tribological test the voluminal fraction is represented according to the applied normal load Fn (fig. 13-b). The found results show that the beneficial effect of films to resist wear is detected for applied loads $F_n \leq 5N$, high this value one brings closer more and more the tribological behavior of the two antagonists in contact alumine/substrat, from where the beneficial effect of films is detected for the weak applied loads.

4. Conclusion

We synthesized coatings having a composition report of N/Cr close to 1 with a dual magnetron for 20% of nitrogen in plasma. These coatings are well crystallized. Analyses XPS and SIMS showed that the multi-layer coatings carried out by pulverization magnetron present quite clear interfaces between the mono-layers and who do not present inter-diffusion substrate-coating. A good homogeneity of the layers on all their depth was highlighted. In addition, the oxygen contamination of the multi-layer coatings is minimal, less than 5% at in volume on a few ten nanometer of depth. The analyses by x-rays diffraction highlighted the strong texture of the multi-layer deposits CrN/CrAlN and Cr/CrN/CrAlN, which is the consequence of the high residual stresses in the mono-layers. These constraints are decreased in the multi-layers under the effect of the interfaces presented in film. Moreover, the thermal properties of multi-layer are refined under the presence of the surface layer CrAlN, which plays the role of a thermal barrier. In addition, all the multi-layers developed in this work have a good adherence with steel 42CrMo4, and adhesion is better in the case of presence of an underlayer Cr (P_T) in film.

5. References

[1] H.A. Jehn, M.E. Baumggartner, *Surf. Coat. Technol.* 108, 54-55 (1992)
[2] M. Panjan, S. Šturm, P. Panjan, M. Čekada, *Surf. Coat. Technol.* 202, 815-819 (2007)
[3] L.A. Dobrzański, M. Polok, M. Adamiak, *Journal of Materials Processing Technology* 164-165, 843-849 (2005)
[4] Youn J. Kim, Tae J. Byun, Jeon G.Hon, *Superlattices and Microstructures* 45, 73-79 (2009)
[5] P.H. Mayrhofer, H. Willmann, C. Mitterer, *Surf. Coat. Technol*. 222, 146 -147 (2001)
[6] M. Kawate, A.K. Hashimoto, T. Suzuki, *Surf. Coat. Technol.* 165,163 (2003).
[7] Y. C. Chim and al., *Thin Solid films* 517, 4845- 4849 (2009)
[8] M. Uchida, N. Nihira, A. Mitsuo, K. Toyoda, K. Kubota, T. Aizawa, *Surf. Coat. Technol.* 627, 177-178 (2004).
[9] L. WANG et al. Surf. Coat. Technol. (2010).
[10] MAGNUS Odén, CLAES Ericsson, GREGER Hakansson, HENRIK Ljunerantz, Surf. Coat. Technol. 114(1999)39-51
[11] B. TLILI, Mustapha. NASRI, C. Nouveau, Y. BENLATRECHE, G. GUILLEMO, M. LAMBERTIN, Vacuum 84 (2010) 1067-1074
[12] C. NOUVEAU, Thèse de doctorat n°21-2001, ENSAM de Cluny
[13] C. NOUVEAU, M. A. DJOUDI, C. DECES-PETIT, Surf. Coat. Technol.174-175 (2003)-455.
[14] B. WARCHOLINSKI, A. GILEWICZ, Z. KUKLINSKI, P. MYSLINSKI, Surf. Coat. Technol. 204(2010), 2289-2293.

[15] Harish C. BARSHILIA, B. DEEPTHI, N. SELVAKUMER, Anja JAIN, K.S. RAJAM; Applied Surface Science 253 (2007) 5076-5083.
[16] A. LIPPITZ, T. HUBERT. Surf. Coat. Technol. 200 (2005) 250.
[17] H.C. BARSHILIA et al. Surface & Coatings Technology 201 (2006) 2193-2201
[18] K. J. Lee, J. W. Kang, P. S. Jeon, H. J. Kim, J. Yoo, Thermochimica Acta, 455 (2007) 60–65.
[19] A. LAPPITZ. Th. HUBERT, Surf. Coat. technol. 200 (2005) 250.
[20] S.R PULUGURTHA et al. Surf. Coat. technol. 202 (2007) 755-761.
[21] Taher GHRIB, Sahbi BEN SALEM, Noureddine YACOUBI, Tribology International, Volume 42, Issue 3, March 2009, Pages 391-396.
[22] Taher GHRIB, Noureddine YACOUBI, Faycel Saadallah, Sensors and Actuators A 135 (2007) 346-354.
[23] Li CHEN, Yong DU, S.Q. WANG, Jia LI, International Journal of Refractory Metals & Hard Materials 25 (2007) 400-404.
[24] Yu CHUNYAN, Tian LINHAI, Wei YINGHUI, Wang SHEBIN, Li TIANBAO, Xu BINGSHE, Applied Surface Science 255 (2009) 4033-4038.
[25] J. ALMER, M. ODEN, G. HAKANSSON, Thin Solid Films 385 (2001) 190.

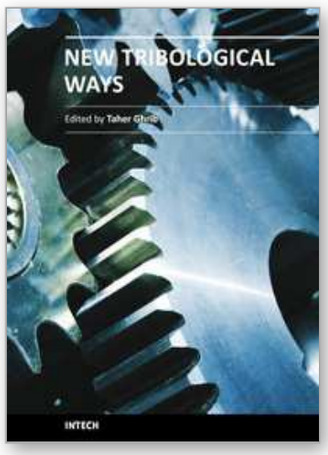

New Tribological Ways

Edited by Dr. Taher Ghrib

ISBN 978-953-307-206-7
Hard cover, 498 pages
Publisher InTech
Published online 26, April, 2011
Published in print edition April, 2011

This book aims to recapitulate old information's available and brings new information's that are with the fashion research on an atomic and nanometric scale in various fields by introducing several mathematical models to measure some parameters characterizing metals like the hydrodynamic elasticity coefficient, hardness, lubricant viscosity, viscosity coefficient, tensile strength .... It uses new measurement techniques very developed and nondestructive. Its principal distinctions of the other books, that it brings practical manners to model and to optimize the cutting process using various parameters and different techniques, namely, using water of high-velocity stream, tool with different form and radius, the cutting temperature effect, that can be measured with sufficient accuracy not only at a research lab and also with a theoretical forecast. This book aspire to minimize and eliminate the losses resulting from surfaces friction and wear which leads to a greater machining efficiency and to a better execution, fewer breakdowns and a significant saving. A great part is devoted to lubrication, of which the goal is to find the famous techniques using solid and liquid lubricant films applied for giving super low friction coefficients and improving the lubricant properties on surfaces.

How to reference

In order to correctly reference this scholarly work, feel free to copy and paste the following:

Tlili Ibrahim and Taher Ghrib (2011). Study of CrAlN Multilayred Thin Films, New Tribological Ways, Dr. Taher Ghrib (Ed.), ISBN: 978-953-307-206-7, InTech, Available from: http://www.intechopen.com/books/new-tribological-ways/study-of-craln-multilayred-thin-films

INTECH
open science | open minds

InTech Europe
University Campus STeP Ri
Slavka Krautzeka 83/A
51000 Rijeka, Croatia
Phone: +385 (51) 770 447
Fax: +385 (51) 686 166
www.intechopen.com

InTech China
Unit 405, Office Block, Hotel Equatorial Shanghai
No.65, Yan An Road (West), Shanghai, 200040, China
中国上海市延安西路65号上海国际贵都大饭店办公楼405单元
Phone: +86-21-62489820
Fax: +86-21-62489821

IntechOpen